

# Lawrence Berkeley National Laboratory

## Lawrence Berkeley National Laboratory

### Title

Impact of land use change on the local climate over the Tibetan Plateau

### Permalink

<https://escholarship.org/uc/item/6px6p25n>

### Author

Jin, J.

### Publication Date

2010-08-09

Peer reviewed

# **Impact of Land Use Change on the Local Climate Over the Tibetan Plateau**

Jiming Jin

Departments of Watershed Sciences & Plants, Soils, and Climate, Utah State University,  
Logan, Utah

Shihua Lu and Suosuo Li

Cold and Arid regions Environmental and Engineering Research Institute, Chinese  
Academy of Sciences, Lanzhou, China

Norman L. Miller

Department of Geography, University of California at Berkeley, California &  
Earth Sciences Division, Lawrence Berkeley National Laboratory, Berkeley, California

## **Abstract**

Observational data show that the remotely sensed leaf area index (LAI) has a significant downward trend over the east Tibetan Plateau (TP), while a warming trend is found in the same area. Further analysis indicates that this warming trend mainly results from the nighttime warming. The Single Column Atmosphere Model (SCAM) version 3.1 developed by the National Center for Atmospheric Research is used to investigate the role of land use change in the TP local climate system and isolate the contribution of land use change to the warming. Two sets of SCAM simulations were performed at the Xinghai station that is located near the center of the TP Sanjiang (three rivers) Nature Reserve where the downward LAI trend is largest. These simulations were forced with the high and low LAIs. The modeling results indicate that when the LAI changes from high to low, the daytime temperature has a slight decrease, while the nighttime temperature increases significantly, which is consistent with the observations. The model further indicates that the nighttime temperature increase results from the less downward sensible heat flux that remains more energy in the near surface boundary layer and increases the temperature there. The more stable boundary layer is caused by the lower surface roughness length in the low LAI case than in the high LAI case. This modeling

study gives a strong insight into future modeling and observational studies for climate change in this high elevation area.

## 1. Introduction

It has become apparent that climate change over high-elevation regions is occurring at a faster rate than over low-elevation regions (Diaz and Bradley 1997). This high-elevation rate of change often generates stronger disturbances within the climate system than low elevation changes (Jin and Miller 2006). The Tibetan Plateau (TP) is an immense upland area (3500 x 1500 km), with an average elevation greater than 5,000 m. Over the TP, 46% of the forest cover and 50% of the grassland have been converted to farmland, urban areas, or desert during the last century (X. Liu, personal communication). The TP is the source of snowmelt runoff, supplying water resources to users in China, India, and surrounding areas. The mechanisms influencing the observed rapid climate change and their impacts at this high elevation region are not well understood. In order to reduce these types of uncertainties and provide society with more reliable projections of future outcomes, detection and analysis of these processes need to be determined.

Many researchers have shown that land use and land cover change, most significantly agricultural change, interacts with the climate system (Cui et al. 2006; Li and Xue 2010). Christy et al. (2006) performed a statistical analysis of the southern half of the Central Valley using high-quality temperature observations for evaluating the role of land use that has changed dramatically due to extensive agricultural expansion since the pre-settlement (circa 1860s). Their study indicated that the daily maximum near-

surface air temperature exhibited a cooling trend over the last century for this region. This finding is opposite to the observed warming trends that prevail over most other regions (Hansen et al. 2006; Houghton et al. 2001; many others), suggesting that agricultural activity and associated irrigation processes most likely play a key role in producing this cooling trend. Modeling studies have shown that such land use change affects regional climate by altering the components in the surface energy budget (Kueppers et al. 2006). Based on the results from a general circulation model (GCM), Snyder et al. (2004) indicate that removing all temperate forest and replacing it with bare soil will produce cooling in the winter and spring over tropical and boreal areas due to an increase in the surface albedo, but a warming during the summer due to reduced evapotranspiration. If forced with a moderate amount of carbon dioxide, GCMs could produce similar results for the entire 21st century (Feddema et al. 2005). These GCM predictions also indicate that the response of land use change could be overridden by a strong atmospheric circulation system such as the Asian Monsoon circulation.

However, due to the lack of detailed long-term and densely distributed spatial observations, researchers have not been able to determine how and to what extent these land use changes affect the early and accelerated warming observed on the TP (Frauenfeld et al. 2005). A high-quality climate model is an efficient tool to advance our understanding of this problem, and observed climate change could be quantitatively interpreted through the model details. The modeling results would further yield new insight into future field experimental design. Therefore, in this study, we use the Single Column Atmosphere Model (SCAM) version 3.1 coupled with the Community Land

Model version 3 (<http://www.cesm.ucar.edu/models/atm-cam/docs/scam/>) to investigate the role of land use change in the TP local climate system and isolate the contribution of land use change to the warming of the TP from that of greenhouse gas emissions. The SCAM was developed by the National Center for Atmospheric Research (NCAR). In addition, the mechanisms associated with land use change signals are adequately quantified with the model output and our existing quality-controlled observations.

## 2. Model, Data, and Methodology

The SCAM used in this study is a one-dimensional time-dependent single column atmospheric model. The SCAM is embedded in the NCAR Community Atmospheric Model version 3. Since the SCAM includes only one model grid cell, it can be used to effectively study land-atmosphere interactions. This grid cell can include up to 10 land use types, giving a benefit to characterize land surface heterogeneity. In this study, the land use types are prescribed in the SCAM to represent land surface features in the TP. The SCAM is also configured with 26 vertical layers ranging from approximately 3 mb to the surface, and it includes all the physical schemes existing in its global counterpart, CAM3. The reanalyzed data by National Centers for Environmental Prediction (NCEP-R1) provide the initial and lateral boundary conditions for SCAM. The latter were updated every 6 hours. The initial conditions include soil moisture and temperature and atmospheric pressure, moisture, temperature, and winds. The 16 km resolution Advanced Very High Resolution Radiometer (AVHRR) leaf area indices (LAIs) were used to examine vegetation changes over the TP and also were inputted into SCAM to more

realistically reflect vegetation variations. Station observations were used to analyze climate change over the TP and compare with modeling results.

### 3. Results

#### 3.1 LAI, temperature, and precipitation analysis

Land use and land cover on the TP has been changed significantly. Such change can be identified with the AVHRR LAI trends over the period of 1983-2000 for July, August, and September, a season that the LAIs usually reach their maximum values (Figure 1). It is clearly seen that the LAIs have negative trends (blue colors) in the northeast TP, with the maximum trend exceeding  $-1.0/\text{decade}$ . These trends are calculated through a linear regression method. The region with the negative trends contains the headwaters of the Yellow River (Huang He), the Yangtze River (Chang Jiang), and the Mekong River (Lancang Jiang), providing a significant amount of water resources to China and Southeast Asia. This area is also called Sanjiang (three rivers) Headwaters Nature Reserve. In some locations of the southeast TP, LAIs also show positive trends (red colors). Figure 2 shows the time series of the annual maximum LAI at a station called Xinghai that is located near the center of the Sanjiang area. This figure shows that the annual maximum LAI has a downward trend with a value of  $-0.67/\text{decade}$  over the period of 1983-2000. According to the United States Geological Survey data, Xinghai has a flat terrain and mostly is covered by grassland during the summer. All the following simulations were performed at this station to understand how vegetation affects local climate.

Figure 3a shows the time series of the annual precipitation anomalies at the Xinghai station for the period of 1960-2000. It is shown that the trend is 0.5 mm/decade, which is quite insignificant. However, the annual mean temperature trend is 0.25 °C/decade (Figure 3b). The temperature increase is about 1 °C at this station over the study period. When temperatures at 2 AM and 2 PM are examined, it can be seen that the nighttime temperature trend is 0.35 °C/decade (Figure 3c) while the daytime temperature trend is only 0.04 °C/decade (Figure 3d). Thus, the annual mean temperature increase results from the nighttime warming. Identifying physical factors and processes that contribute to the nighttime warming is the major focus of the following sections, where we use the SCAM model for a controlled analysis and sensitivity study.

### 3.2 SCAM evaluation

Before physical processes that affect temperature change are studied, the SCAM needs to be fully evaluated with observations to ensure that it can reasonably describe climate processes in our study area. SCAM simulations at the Xianghai station were performed over the period of 1951-2000. The first 32-year (1951-1982) simulations were discarded for spinning up the model, and only the simulations over the period of 1983-2000 were analyzed. Figure 4a shows that although the SCAM produces a weaker seasonal cycle of the temperature, it still generates reasonable temperature simulations at the Xinghai station when compared to the observations. The correlation coefficient between the observation and the simulation is 0.98, the RMSE is 2.2 °C, and the bias is 0.29 °C. The model can also reproduce the observed precipitation, where the correlation coefficient, and RMSE, and bias is 0.74, 28mm/month, and 13 mm/month, respectively (Figure 4b).

These results show that the SCAM well simulates the seasonal cycles of precipitation and temperature at the Xinghai station, indicating that this model can be used to further explore physical processes that affect temperature and precipitation changes in this area.

### 3.3 Sensitivity studies for understanding the temperature changes.

To examine how vegetation affects the warming in this area, two additional sets of simulations were performed with high and low LAIs for 1983-2000, a period where the remotely sensed LAIs are available. Figure 5 shows seasonal variations of high and low LAIs. The high LAIs are the average over the 1983-1985, while the low LAIs are the average over 1998-2000. The largest difference between the high and low LAIs is more than one. The first set of simulations was forced with the high LAIs, where the LAI only varied seasonally but did not have interannual variations. The model settings for the second set of simulations were exactly the same as those for the first, except for the low LAI values. Figure 6a shows the 2 m height temperature difference between the high LAI and the low LAI cases averaged over the 18-year period (1983-2000). It is seen that the major changes in temperature (low LAI minus high LAI) occur in the warm season where the LAI difference between the two cases is the largest. During the cold season (from October through next May), there is almost no change for the temperature. Precipitation has very minor changes with a maximum difference of less than 1 mm/month (Figure not shown). Figure 6a indicates that the lower LAI in this region generates a slight cooling during the summer at noontime with a maximum temperature change of  $-0.2^{\circ}\text{C}$  in July (solid line). All the components in the energy balance equation are examined. The results show that the sensible heat flux has most significant changes

that affect 2 m height temperature (Figure 6b). It is seen in the simulation with lower LAI that sensible heat flux decreases by  $10 \text{ W/m}^2$  at noontime during the summer (solid line). Further analysis indicates that such a decrease results from the lower roughness in the low LAI case. In SCAM, the roughness length for vegetation in this area is 0.06 m, and for bare soil, it is 0.024 m. The low LAI reduces the areal weight of vegetation in the model grid cell, but increase the weight of bare soil when compared to the settings in the high LAI case. Thus, on average, the low LAIs generate a flatter surface than the high LAIs, which decrease the upward sensible heat flux during daytime and slightly lower the near surface temperature.

Figure 6a shows the nighttime temperature difference between the low and high LAI cases (low-high), indicating that the near surface temperature increases by more than  $1 \text{ }^\circ\text{C}$  in July due to changing the LAI from high to low (dashed line). During the evening, the sensible heat flux is downward (negative). The reduced roughness length in the low LAI case suppresses the energy exchanges between the surface and near surface air. Figure 6b shows that the increase in sensible heat flux at midnight is up to  $2 \text{ Wm}^2$  (dashed line) that leads to more energy remaining in the near surface air (less downward sensible heat) and increases the temperature there. Detailed calculation of sensible heat flux and how it is related to the roughness length are described in Oleson et al. (2004).

The above modeling results strongly suggest that the warming results from nighttime temperature changes that are consistent with the observations. The decreased vegetation LAI in this area significantly contributes to the nighttime temperature increase. The LAI

decrease may not be a controlling factor that produces the observed warming trend, but most likely it reinforces the existing warming trend that is believed to be triggered by the carbon increase in the atmosphere (Cui et al 2006).

#### 4. Conclusions and Discussions

In northeast Tibetan Plateau, the remotely sensed LAIs show a significant downward trend, while a warming trend is observed for temperature. Our modeling results indicate that such a vegetation change is an important factor that contributes to the warming in this region. Further analysis indicates that this contribution largely comes from the evening temperature increase. The evening temperature increase results from the more stable near-surface boundary layer that restricts the downward sensible heat flux and remains more energy in the near-surface air. The deterioration of vegetation leads to a flatter area reduces the surface roughness, and results in more stable near-surface boundary layer.

This study is not intended to indicate that vegetation deterioration is a determining factor that leads to a warming in this area that is most likely related to global climate change triggered by the atmospheric carbon increase. Instead, the analysis shown in this study describes a fact that the reduced biomass in this area could strengthen the warming trend in this region. This study is based on the modeling results that need to be further verified with more observed evidence. The large- and meso-scale atmospheric information in the SCAM was introduced through the lateral boundary data. Thus, the atmosphere in the model column does not produce any feedback to that outside the

column. Thus, this drawback could be overcome by applying a regional or global climate model to this region, which could be a future research topic. However, these modeling results give strong insight into future modeling and observational studies for climate change in this high elevation area.

Acknowledgements: Support for this work provided by the Utah Agricultural Experiment Station. JJ was also supported by K. C. Wong Fellowships, Chinese Academy of Sciences. Work by N.L. Miller is under the Department of Energy contract number DE-AC02-05CH11231.

#### References:

Christy, R. C., W. B. Norris, K. Redmond, K. P. Gallo, 2006: Methodology and results of calculating central California surface temperature trends: evidence of human-induced climate change? *J. Climate*, 19, 548-563.

Cui, X., H. F. Graf, B. Langmann, W. Chen, R. and Huang, 2006: Climate impacts of anthropogenic land use changes on the Tibetan Plateau. *Glob. Planet. Change*, 54, 33-56.

Diaz, H. F. and R.S. Bradley, 1997: Temperature variations during the last century at high elevation sites. *Climatic Change*, 36, 253-279.

Feddema, J. J., K. W. Oleson, G. B. Bonan, L.O. Mearns, L. E. Buja, G. A. Meehl, and W.M. Washington, 2005: The importance of land cover change in simulating future climates. *Science*. **310**, 1674-1678.

Frauenfeld, O. W., T. Zhang, and M. C. Serreze, 2005: Climate change and variability using European Centre for Medium-Range Weather Forecasts reanalysis (ERA-40) temperatures on the Tibetan Plateau. *J. Geophys. Res.*, 110, D02101, doi:10.1029/2004JD005230.

Hansen J., M. Sato, R. Ruedy, K. Lo, D. W. Lea, and M. Medina-Elizade, 2006: Global temperature change. *Proc. Natl. Acad. Sci.*, 103, 14288-14293.

Houghton, J.T., Y. Ding, D.J. Griggs, P.J. van der Linden, X. Dai, K. Maskell, and C.A. Johnson, 2001: Climate Change 2001: The Scientific Basis. Contribution of Working

Group I to the Third Assessment Report of the Intergovernment Panel on Climate Change, 881pp.

Jin, J., and N. L. Miller, 2006: Toward understanding the role of ground water in hydroclimate over the Merced watershed using a Single Column Climate Model. The 2006 AGU fall meeting, December 11-15, 2006, San Francisco, CA.

Kueppers, L. M., M. A. Snyder, L. C. Sloan, D. Cayan, J. Jin, H. Kanamaru, M. Kanamitsu, N. L. Miller, M. Tyree, H. Du, and B. Weare, 2008: Seasonal temperature responses to land-use change in the western United States. *Global and Planetary Change*, 60: 250-264.

Li, Q., and Y. Xue, 2010: Simulated impacts of land cover change on summer climate in the Tibetan Plateau. *Environ. Res. Lett.* 5 015102, doi: 10.1088/1748-9326/5/1/015102.

Oleson, K.W., Y. Dai, G. Bonan, M. Bosilovich, R. Dickinson, P. Dirmeyer, F. Hoffman, P. Houser, S. Levis, G.-Y. Niu, P. Thornton, M. Vertenstein, Z.-L. Yang, and X. Zeng, 2004: Technical Description of the Community Land Model (CLM), NCAR/TN-461+STR, 174pp.

Snyder, P. K., C. Delire, J. A. Foley, 2004: Evaluating the influence of different vegetation biomes on the global climate. *Climatic Dynamics*. 23, 279-302. DOI: 10.1007/s00382-004-0430-0.

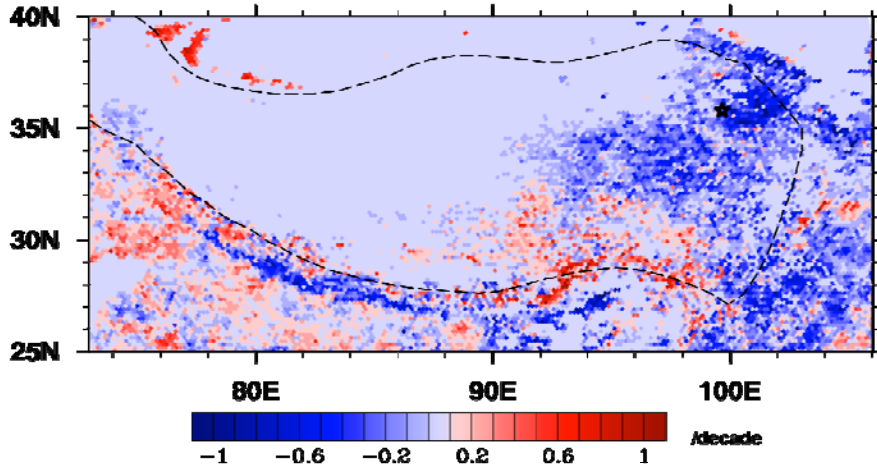


Figure 1 The LAI trend in the TP over the period of 1983-2000 (unit: /decade). The dashed line represents the scope of the TP. The black star is the location of the Xinghai station where the SCAM simulations were performed.

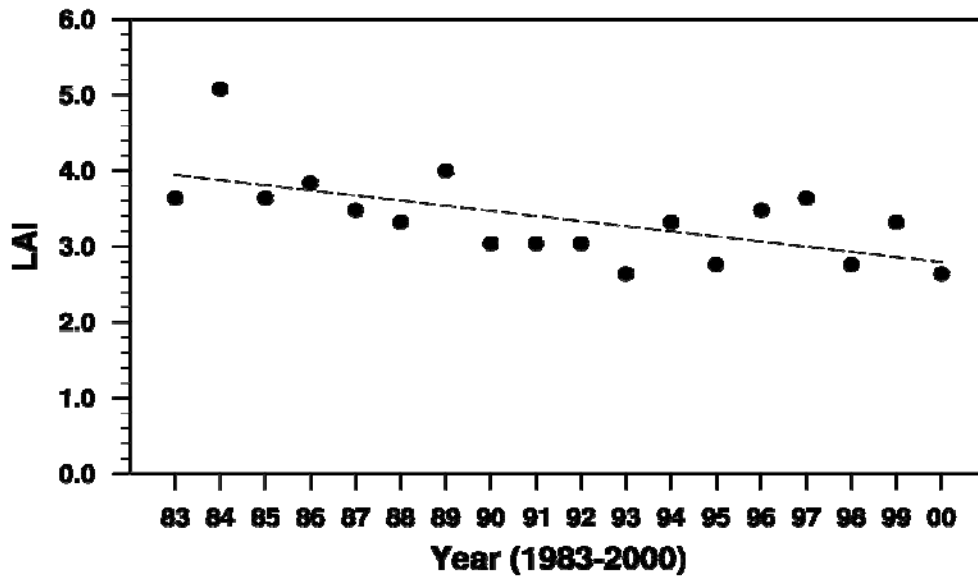


Figure 2 The trend of the annual maximum LAI at the Xinghai station for the period of 1983-2000. The dashed line represents the trend. The black dot is the maximum LAI for each year.

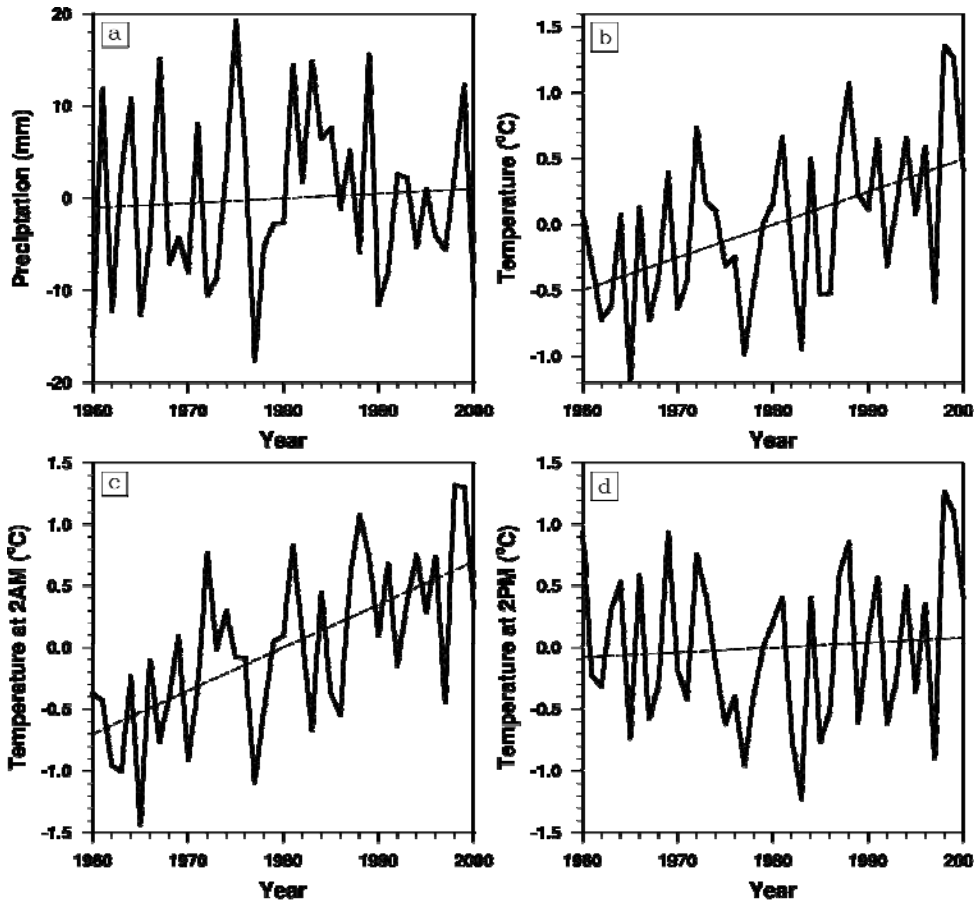


Figure 3 The time series of annual precipitation and temperature anomalies at the Xinghai station. a) precipitation (mm); b) temperature (°C); c) temperature at 2 AM (°C); temperature at 2 PM. The dashed line in each figure represents the trend.

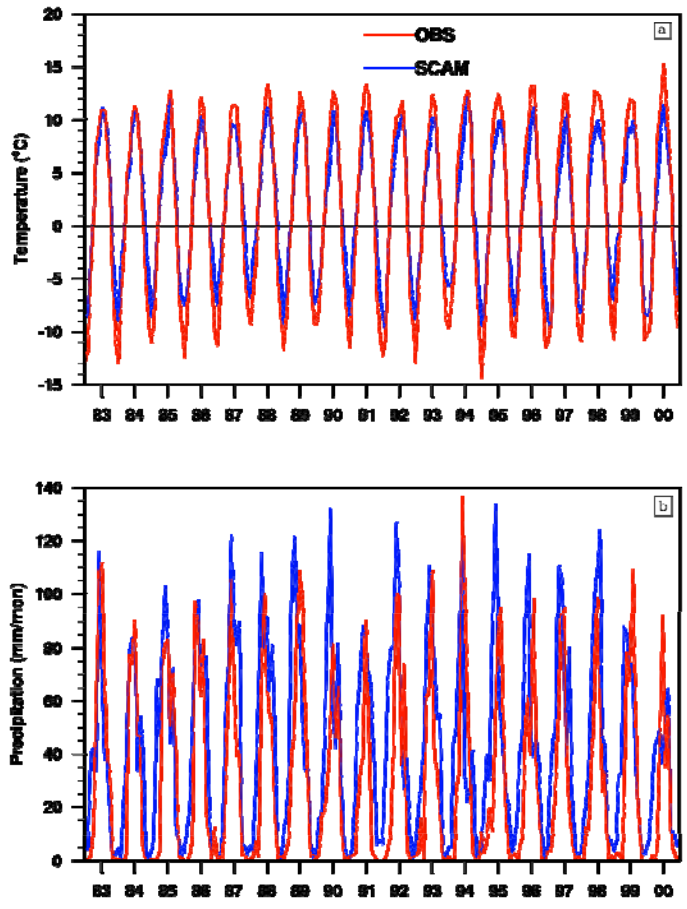


Figure 4. Comparison of SCAM simulations (blue line) and observations (red line) at the Xinghai station. a) precipitation; b) temperature.

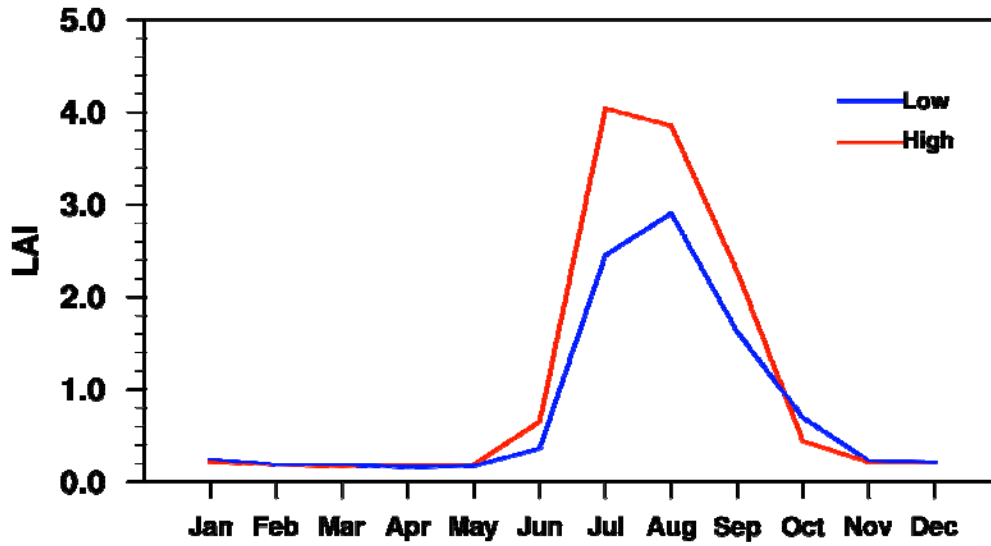
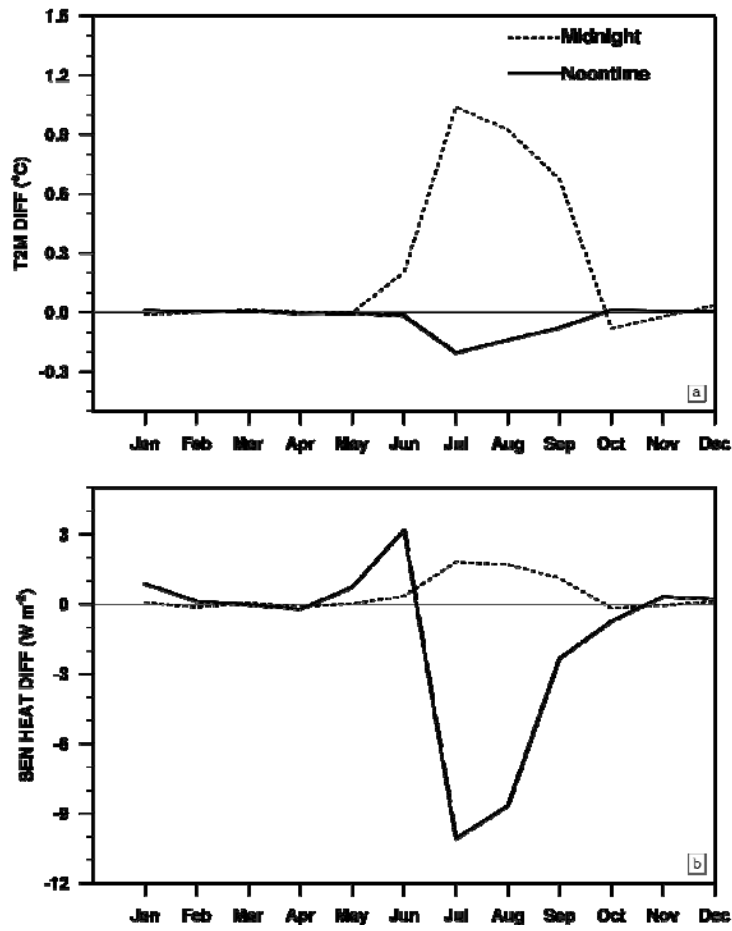


Figure 5 The seasonal variations of the low (blue) and high (red) LAIs. The high LAI is the average over 1983-1985, while the low LAI is the average over 1998-2000.



a

Figure 6 The a) temperature (unit:  $^{\circ}C$ ) and b) sensible heat flux (unit:  $W m^{-2}$ ) differences between the low and high LAI cases (low-high). The solid line is for noontime, and the dashed line is for midnight.